Journal of Cell Science 109, 837-849 (1996)
Printed in Great Britain © The Company of Biologists Limited 1996
JCS7024

Microtubule-based peroxisome movement

Stephan Rapp[1,*], Rainer Saffrich[2], Markus Anton[1], Ursula Jäkle[1], Wilhelm Ansorge[2], Karin Gorgas[3] and Wilhelm W. Just[1,†]

[1]Institut für Biochemie I der Universität Heidelberg, Im Neuenheimer Feld 328, D-69120 Heidelberg, Germany
[2]EMBL, Heidelberg, Germany
[3]Institut für Anatomie und Zellbiologie II der Universität Heidelberg, Heidelberg, Germany

*Present address: Abteilung für Angewandte Tumorvirologie, Deutsches Krebsforschungszentrum, Heidelberg, Germany
[†]Author for correspondence
Parts of this work were presented at the International Symposium 'Peroxisomes: Biology and Role in Toxicology and Disease', held in Aspen, Colorado, 1995

SUMMARY

The association of peroxisomes with cytoskeletal structures was investigated both by electron microscopy and by kinetic analysis of peroxisome movement. The morphological studies indicated distinct interactions of peroxisomes with microtubules and frequently revealed multiple contact sites. The kinetic approach utilised microinjection and import of fluorescein-labeled luciferase in order to mark and track peroxisomes in vivo. Peroxisomal motility was analysed by time-lapse imaging and fluorescence microscopy. According to their movement peroxisomes were classified into two groups. Group 1 peroxisomes comprising the majority of organelles at 37°C moved slowly with an average velocity of 0.024±0.012 μm/second whereas the movement of group 2 peroxisomes, 10-15% of the total population, was saltatory exhibiting an average velocity of 0.26±0.17 μm/second with maximal values of more than 2 μm/second. Saltations were completely abolished by the microtubule-depolymerising drug nocodazole and were slightly reduced by about 25% by cytochalasin D which disrupts the actin microfilament system. Double fluorescence labeling of both peroxisomes and microtubules revealed peroxisome saltations linked to distinct microtubule tracks. Cellular depletion of endogenous levels of NTPs as well as the use of 5′-adenylylimidodiphosphate, a nonhydrolysable ATP analog, applied to a permeabilised cell preparation both completely blocked peroxisomal movement. These data suggest an ATPase dependent, microtubule-based mechanism of peroxisome movement. Both the intact and the permeabilised cell system presented in this paper for the first time allow kinetic measurements on peroxisomal motility and thus will be extremely helpful in the biochemical characterisation of the motor proteins involved.

Key words: Peroxisome motility, Microtubule, Actin filament, ATP-dependence

INTRODUCTION

Since the observation of Goldfischer et al. (1973) who identified the cause of the cerebro-hepato-renal syndrome of Zellweger as a defect in peroxisome biogenesis (for reviews see Schutgens et al., 1986; Roscher and Rolinski, 1992) peroxisome research mainly focused on targeting and import of peroxisomal matrix proteins (for a review see Subramani, 1993), the insertion of proteins into the peroxisomal membrane (Diestelkötter and Just, 1993), and the identification of membrane components participating in the biogenesis of peroxisomes (McCammon et al., 1990; Tsukamoto et al., 1991; Höhfeld et al., 1991; Shimozawa et al., 1992; Allen et al., 1994; Tan et al., 1995; Erdmann and Blobel, 1995). Besides the biogenetic aspects on targeting and import of peroxisomal proteins there are other intriguing questions concerning the biogenesis of peroxisomes such as for example the generation and maintenance of size and shape of peroxisomes, the formation of new peroxisomes, the maintenance of their cytoplasmic distribution or the control of their degradation. In higher eukaryotes only liver and kidney contain large spherical peroxisomes of about 0.5 μm in average diameter. In most other organs peroxisomes are of a more tubular structure resembling the endoplasmic reticulum (Gorgas, 1984, 1985). There is strong biochemical evidence that new peroxisomes are formed by budding and fission from parent organelles (for a review see Lazarow and Fujiki, 1985) although the underlying mechanisms are not clear and thus far could not be proved experimentally. Peroxisomes in most higher eukaryotic cells seem to be distributed throughout the cytoplasm with no preferential location. On the other hand lysosomes, which are the compartment of final peroxisomal degradation, are preferentially found in juxtaposition to the cell nucleus (Matteoni and Kreis, 1987).

Analogous to other organelles some of these biogenetic aspects may be intimately related to the functions of the cytoskeleton. For example microtubules have been shown to be involved in the organization of the endoplasmic reticulum (Dabora and Sheetz, 1988; Allan and Vale, 1994), the Golgi apparatus (Rogalski and Singer, 1984; Marks et al., 1994) and the endosomal compartment (Bomsel et al., 1990; Aniento et al., 1993). Cell organelles move along cytoskeletal tracks and are driven by microtubule- and/or actin-based motor enzymes (for reviews see Schliwa, 1984; Walker and Sheetz, 1993;

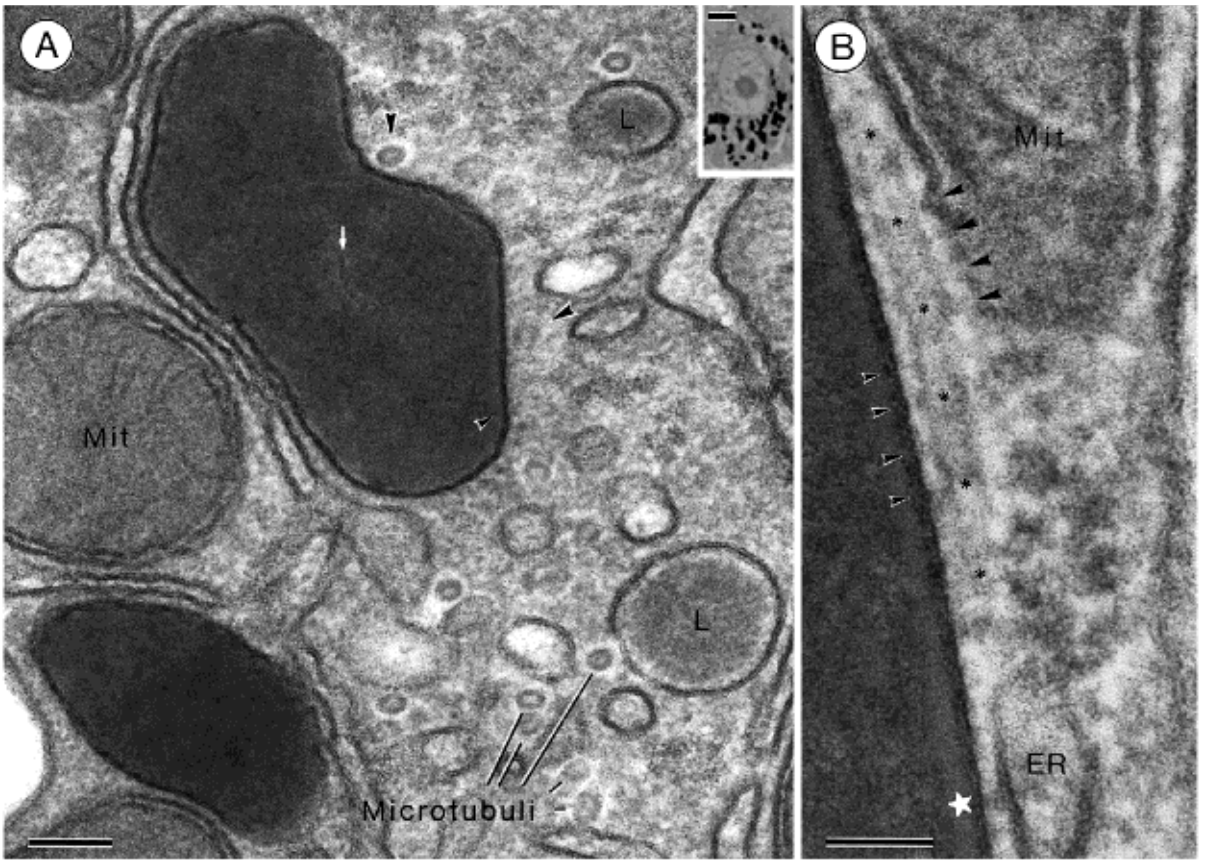

Fig. 1. Light and electron micrographs of tubular epithelial cells of the P_3-segment of canine nephron incubated for catalase activity. (Inset in A) Peroxisomes are abundant and clustered in the basolateral cytoplasm. (A) Microtubules are frequently seen in close association with lysosomes (L) and ER-profiles as well as peroxisomes (large arrowheads). (B) Over a rather long distance a microtubule (small black asterisks) is decorated with numerous filamentous side-arms forming cross-bridges to a peroxisome (small arrowheads) and a mitochondrium (large arrowheads). Note the filamentous matrical inclusions (white arrow in A) and the marginal plates (small arrowhead in A and white asterisk in B). Tubular profile of the endoplasmic reticulum (ER), Mit, mitochondrium. Bars: 3 μm (inset in A); 100 nm (A); 50 nm (B).

Langford, 1995). These data strongly suggest that such cytoskeletal interactions may also exist for peroxisomes and may play an important role in their biogenesis. Therefore, in the present study, we analysed in detail the peroxisomal-cytoskeletal associations at the electron microscope level in appropriate tissues and established an in vivo system allowing the continuous observation of peroxisomes within the living cell. Based on our recent findings that firefly luciferase (FL) upon microinjection is imported into peroxisomes of various mammalian cell lines (Soto et al., 1993) we were able to visualise and track peroxisome movement, and for the first time we report on the spatial and temporal characteristics of intracellular peroxisome movement in vivo. Our data provide evidence for a specific interaction of peroxisomes with cytoskeletal elements, particularly the microtubule system.

MATERIALS AND METHODS

Light and electron microscopy

Perfusion fixation, cytochemical staining, postfixation as well as embedding of the tissue specimens was carried out as described previously (Gorgas, 1984, 1985; Zaar et al., 1984).

Cell culture

CHO wild-type cells (ATCC, Rockville, USA), free of mycoplasma contamination, were grown in 10 cm Falcon plastic dishes in α-MEM (Sigma) supplemented with 7.5% fetal bovine serum and penicillin and streptomycin at a concentration of 10,000 U and 10 mg per 100 ml medium, respectively. Cells were detached from the substratum with trypsin/EDTA 24 hours before microinjection and 1×10^5 cells per 2 ml of medium were transferred to a 3.5 cm Nunc plastic dish with a central borehole of 10 mm diameter to which a 13 mm diameter coverslip was mounted from the outside with ordinary glue. The glue was allowed to harden for at least 24 hours before UV-sterilization of the plastic dishes.

Fluorescence labeling of FL and tubulin

FL (isolated from the firefly *Photinus pyralis*; Boehringer) was dissolved at 0°C at a concentration of 4 mg/ml in microinjection buffer consisting of 48 mM K_2HPO_4, 4.5 mM KH_2PO_4, 14 mM NaH_2PO_4, pH 7.2. To 100 μl of this solution 6 μl of a 5,6-carboxy-fluorescein-*N*-hydroxysuccinimide ester (Fluos; Boehringer) solution (1.54 mg/ml in DMSO) was added, corresponding to a molar ratio of FL to Fluos of 1:3. After 20 minutes at room temperature in the dark unbound label was removed by Sephadex G50 chromatography using the microinjection buffer for elution. Approximately 50% of the label remained covalently bound to the protein resulting in a FL solution of about 2.5 mg/ml with about 1.5 mole of label per mole of protein. This solution was freshly prepared and care was taken to keep the time between labeling and microinjection as short as possible due to the tendency of Fluos-FL to form aggregates which may block the microinjection capillary.

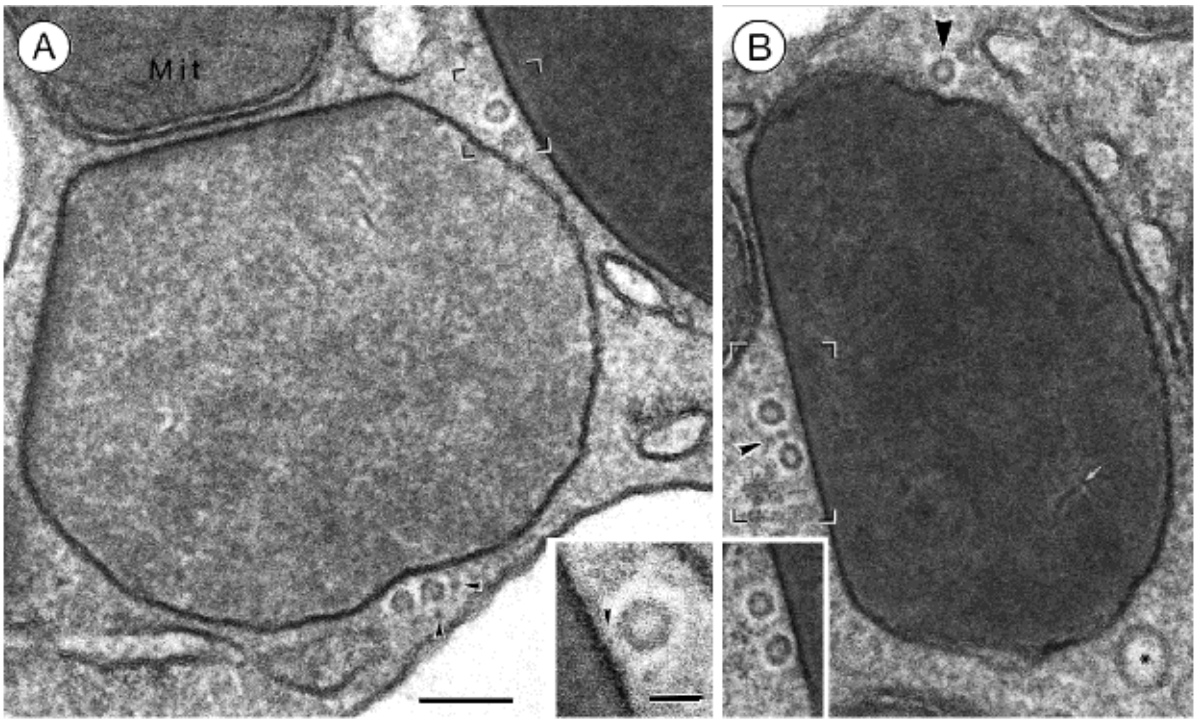

Fig. 2. Electron micrographs of marginal plate-containing peroxisomes located in the basolateral portion of tubular epithelial cells of the P_3-segment of the canine nephron incubated for catalase activity. (A) Peroxisomes are frequently seen in close association with two or even three microtubules. Near the plasma membrane these adjacent microtubules interact with thick filaments (arrowheads). (Inset in A) At higher magnification (region indicated in A) the filamentous cross-bridge linking the microtubule to the peroxisomal membrane is clearly seen. This side arm exhibits a counterclockwise orientation. (B) Serial sections (S_1=B, S_4=inset in B) clearly demonstrate the parallel course of two microtubules which are closely attached to the peroxisomal membrane and separated from each other by a thin cytoplasmic strand (small arrowhead). A third microtubule is in close contact with a distant portion of the peroxisomal membrane (large arrowhead). Note the filamentous matrical inclusions (white arrow) and the uncoated vesicle (asterisk) adjacent to the peroxisomal membrane. Bars: 100 nm (A,B, inset in B); 25 nm (inset in A).

For the simultaneous visualisation of peroxisomes and microtubules in the living cell, monomeric tetramethylrhodamin B isothiocyanate (TRITC)-labeled bovine brain tubulin was coinjected with Fluos-FL. The labeled tubulin (10 mg/ml) was prepared exactly as described previously (Hyman et al., 1991). For coinjection TRITC-labeled tubulin and Fluos-FL were mixed at a 1:1 ratio and applied to Sephadex G50 chromatography at 4°C using 50 mM potassium glutamate, 0.5 mM $MgCl_2$, pH 6.8 for elution. The obtained solution was directly applied for microinjection. With respect to the dynamic instability of microtubules in the double-labeling experiment time-lapse imaging was carried out preferably 10-12 hours after microinjection.

Microinjection

For microinjection the Eppendorf microinjector 5242 and the Eppendorf Micromanipulator 5171 (Eppendorf, Hamburg) were used, the latter being mounted on an Axiovert 35 reversed fluorescence microscope (Zeiss, Oberkochen) as described by Ansorge and Pepperkok (1988). Capillaries for injection were prepared from glass tubings (GC 120 TF-10, Clark Electromedical Instruments, Pangbourne, UK) using the capillary puller model P 87 of Sutter Instruments (Novato, CA). Before microinjection the cell culture medium was replaced by PBS which in turn was exchanged for new medium after injection. Approximately 100 cells per coverslip were injected. The cells were cultured overnight which considerably reduced the background fluorescence caused by the nonimported labeled enzyme.

Application of inhibitors

To study the interaction of peroxisomes with various cytoskeletal components cells were treated either with cytochalasin D (1 μg/ml) or with nocodazole (10 μg/ml) 1 hour before time-lapse imaging. Since both toxins were dissolved in DMSO (1% final concentration in the medium), controls were inspected with only the vehicle in the same concentration. Cells were depleted of ATP by a 30 minute incubation with 10 mM NaN_3 and 6 mM 2-deoxyglucose in glucose-free medium at 37°C as described previously (Soto et al., 1993). Streptolysin O (SLO)-permeabilisation of CHO cells (1-1.5 hemolytic units/ml; Bhakdi et al., 1993) and Fluos-FL import was performed exactly as previously reported (Rapp et al., 1993). Briefly, cells were grown on glass coverslips and the washed cells were incubated at room temperature by inverting the coverslip over 30 μl 'import mix' containing 0.03-0.045 hemolytic units of SLO, 1 μg Fluos-FL, 1.7 mM ATP, 0.85 mM GTP, 16.7 mM creatine phosphate (potassium salt) and 6.25 μg creatine kinase in buffer H which consisted of 165 mM potassium acetate, 2 mM magnesium acetate, 2.5 mM dithiothreitol, 1% BSA and 50 mM Hepes/KOH, pH 7.5. Permeabilised cells were depleted of ATP by omitting ATP and the ATP regenerating system and adding to the medium 5′-adenylylimidodiphosphate (AMP-PNP), a nonhydrolysable ATP analog, in a concentration of 1 mM.

Videoanalysis

Fluorescence microscopy and time-lapse imaging was performed on a Zeiss Axiovert 10 inverted microscope at room temperature (20°C) as well as at 37°C. Images were acquired with a Photometrics CH250 cooled CCD camera (1,317×1,035 pixels) controlled by a SUN Microsystems workstation (SUN 10/41) as described by Herr et al.

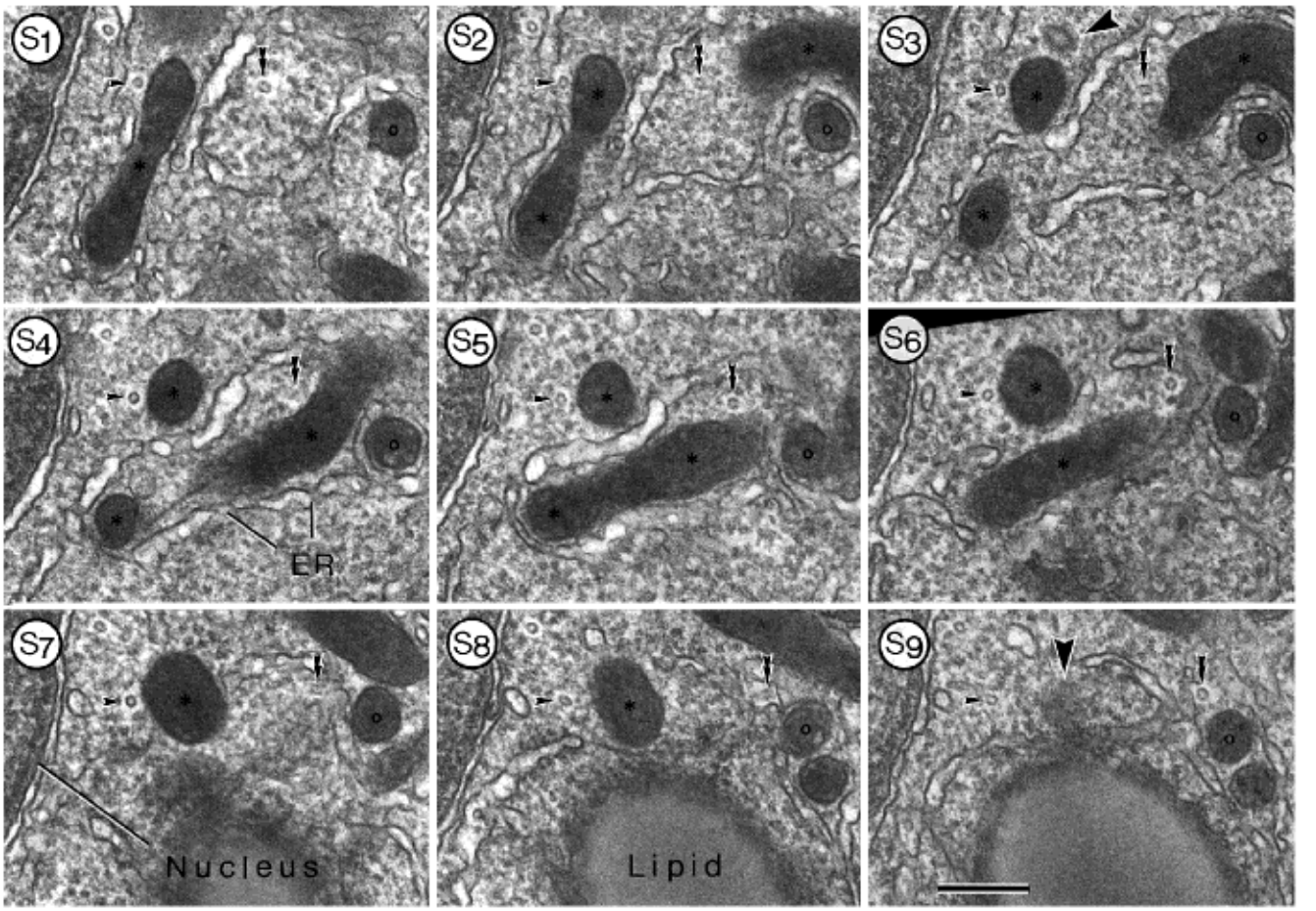

Fig. 3. Electron micrographs of a series of consecutive sections (S_1-S_9) showing the tortuous course of a tubular peroxisome (asterisk) located near the nucleus of a maturing glandular cell of the mouse preputial gland incubated for catalase activity. This series reveals that: two microtubules (arrowhead and double arrowhead) are closely attached to different segments of the organelle; that the 'cap', the definite terminal portion of the organelle (S_8-S_9, note the large arrowhead in S_9) is not directly linked to the adjacent microtubule (arrowhead); and that the two microtubules (arrowhead and double arrowhead) do not display a parallel course. In S_3 note the coated vesicle (large arrowhead) adjacent to the peroxisome (asterisk). Bar, 200 nm (S_1-S_9).

(1993). For the time series, fluorescence images of the microinjected cells were acquired every 30 seconds with an exposure time of 1-2 seconds for each image using a 63-fold magnification objective (Zeiss Plan-Achromat ×63, 1.4). Photobleaching limited the number of images per series to 10-30 images. For analysis of peroxisome motility, the time series were processed and animated with the software package KHOROS (Rasure et al., 1990). Movements were recorded only on peroxisomes that could be observed on all images of a single time series. Displacements were measured as pixel position of the center of a given peroxisome. To calculate the average velocity of peroxisome movements at least 50 organelles of each time series were evaluated. Values are given as means ± s.e.m.

RESULTS

Morphological findings

Peroxisomes of most cell types are rather evenly distributed throughout the cytoplasm. In polarised epithelial cells, however, peroxisomes are localised preferentially in the basolateral region of the cytoplasm (Zaar et al., 1984), often in close association to cytoskeletal structures. In order to examine these associations in more detail we chose the polarised epithelial cells of the P_3-segment of the canine kidney as a model. In these cells peroxisomes are abundant and specifically clustered in the basolateral cytoplasm near the nucleus (inset in Fig. 1A). At the electron microscope level numerous microtubules can be found which are in close proximity not only to peroxisomes, but also to other subcellular organelles, e.g. lysosomes, mitochondria and profiles of the endoplasmic reticulum (Fig. 1A) which all are known to be associated with microtubules. The contacts between mitochondria or axoplasmic vesicles and neurotubules have been determined by many authors to occur usually at a distance of about 10 nm (Smith et al., 1975; Leterrier et al., 1994). A similar close spacing between peroxisomes and their adjacent microtubules is clearly seen in our electron micrographs (Figs 1, 2) particularly in those sections in which a longitudinally traversing microtubule aligns along the peroxisomal membrane (Fig. 1). These close contacts argue for a specific interaction of peroxisomes and microtubules rather than a random distribution.

Microtubules are hollow, nonbranching cylinders which in cross sections appear as ring-like, electron-dense structures

approximately 25 nm in diameter and which are consistently surrounded by a distinct electron-lucent zone (Figs 1, 2). At higher magnification slender projections can be seen radiating from the 5 nm thick microtubular wall. They traverse the electron-lucent space and link the microtubules to adjacent organellar membranes (inset in Fig. 2A). These cross bridges most likely represent motor proteins and/or accessory components mediating the association of organelles to microtubules. In appropriate longitudinal sections in which microtubules parallel the surface of DAB-stained peroxisomes and thus can be followed over a long distance, numerous cross bridges become visible (Fig. 1B). Strikingly, our electron microscope studies of proximal tubular cells revealed more than one microtubule, frequently 2-4, to be in close proximity to peroxisomes (Figs 1A, 2A,B) as well as to mitochondria. In Fig. 2B three microtubules are seen which are closely associated with a single peroxisome. Two of these microtubules are arranged in parallel, situated next to each other and separated by a sheet-like filamentous structure (Fig. 2B and inset in 2B), whereas the third one contacts the same peroxisome at a fairly distant position.

Similar observations also were made in cells of the mouse preputial gland (Fig. 3). The cells of the glandular acinus are subject to differentiation and sebaceous maturation and therefore basal, intermediate and fully differentiated cells can be distinguished which are mainly defined according to their location and the amount of stored lipid. As shown previously (Gorgas, 1984) in the early stages of sebaceous transformation peroxisomes display a striking complex morphological organisation, a kind of branched and extended tubular structure which has been designated as peroxisomal reticulum (Lazarow et al., 1980). The prototype of such tubulovesicular networks is the endoplasmic reticulum, the morphology and function of which, as mentioned above, seems to be strongly affected by its interaction with microtubules. Therefore, the cells of the sebaceous acinus may well serve as a suitable model to study cytoskeletal-peroxisomal interactions. By following the spatial distribution of a tubular peroxisome, typical for a fully differentiated cell, over a distance of nine consecutive serial sections it becomes evident that two microtubules were closely attached to this peroxisome (Fig. 3 and asterisks in Fig. 4). The three-dimensional reconstruction of these serial sections reveals the tortuous structure of the tubular peroxisome and clearly exhibits the nonparallel course of these two microtubules (Fig. 4).

Although these morphological observations strongly suggest a functional interaction of peroxisomes with microtubular structures, they do not prove this interaction. Therefore, we established a system to continuously analyse peroxisome motility. To this end we made use of the specific fluorescence labeling of peroxisomes in vivo that allowed us to record their motility by time-lapse imaging and fluorescence microscopy.

Import of Fluos-FL into peroxisomes of CHO cells

FL in the firefly is a peroxisomal enzyme (Keller et al., 1987). Due to the conserved C-terminal peroxisomal targeting signal SKL (Gould et al., 1987), FL is also imported into mammalian peroxisomes. Recently the import of microinjected FL into peroxisomes of CHO cells was demonstrated by colocalising the FL-based immunofluorescence signal with that of the peroxisomal marker catalase (Walton et al., 1992; Soto et al., 1993; Rapp et al., 1993). In order to label peroxisomes in vivo cells were microinjected with Fluos-FL. This marker is imported into peroxisomes, as clearly demonstrated both by recording the immunofluorescence pattern of labeled FL using a polyclonal rabbit anti-FL antiserum (not shown) and more directly by taking advantage of the fluorophore labeling itself (Fig. 5). A distinct peroxisomal punctate fluorescence pattern is seen (Fig. 5A) which perfectly colocalises with the distribution of

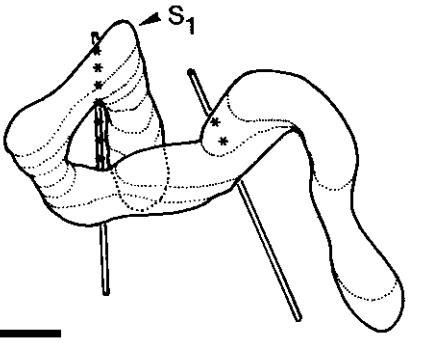

Fig. 4. Schematic three-dimensional reconstruction of the serial thin sections shown in Fig. 3. Note the tortuous structure of the tubular peroxisome and its close association with two microtubules which clearly exhibit a nonparallel course. Asterisks indicate contact sites between microtubules and the peroxisome. Bar, 200 nm.

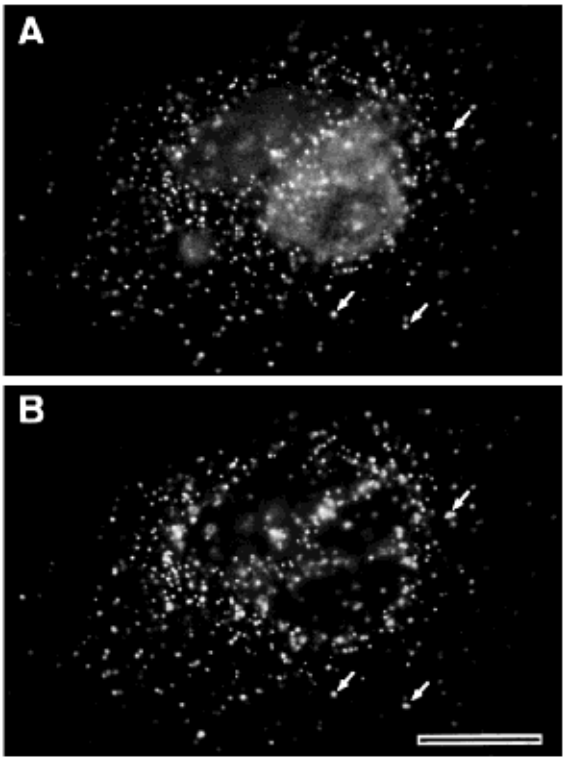

Fig. 5. Peroxisomal localisation of Fluos-FL after microinjection into cultered CHO-cells. The labeled enzyme revealed a punctate fluorescence pattern (A) which perfectly colocalised with the intracellular distribution pattern of catalase, the endogenous peroxisomal marker (B). Catalase distribution was visualised by immunofluorescence using a polyclonal rabbit anti-catalase antiserum and a TRITC-labeled secondary antibody. Arrows mark some of the colocalising peroxisomal structures. Bar, 20 μm.

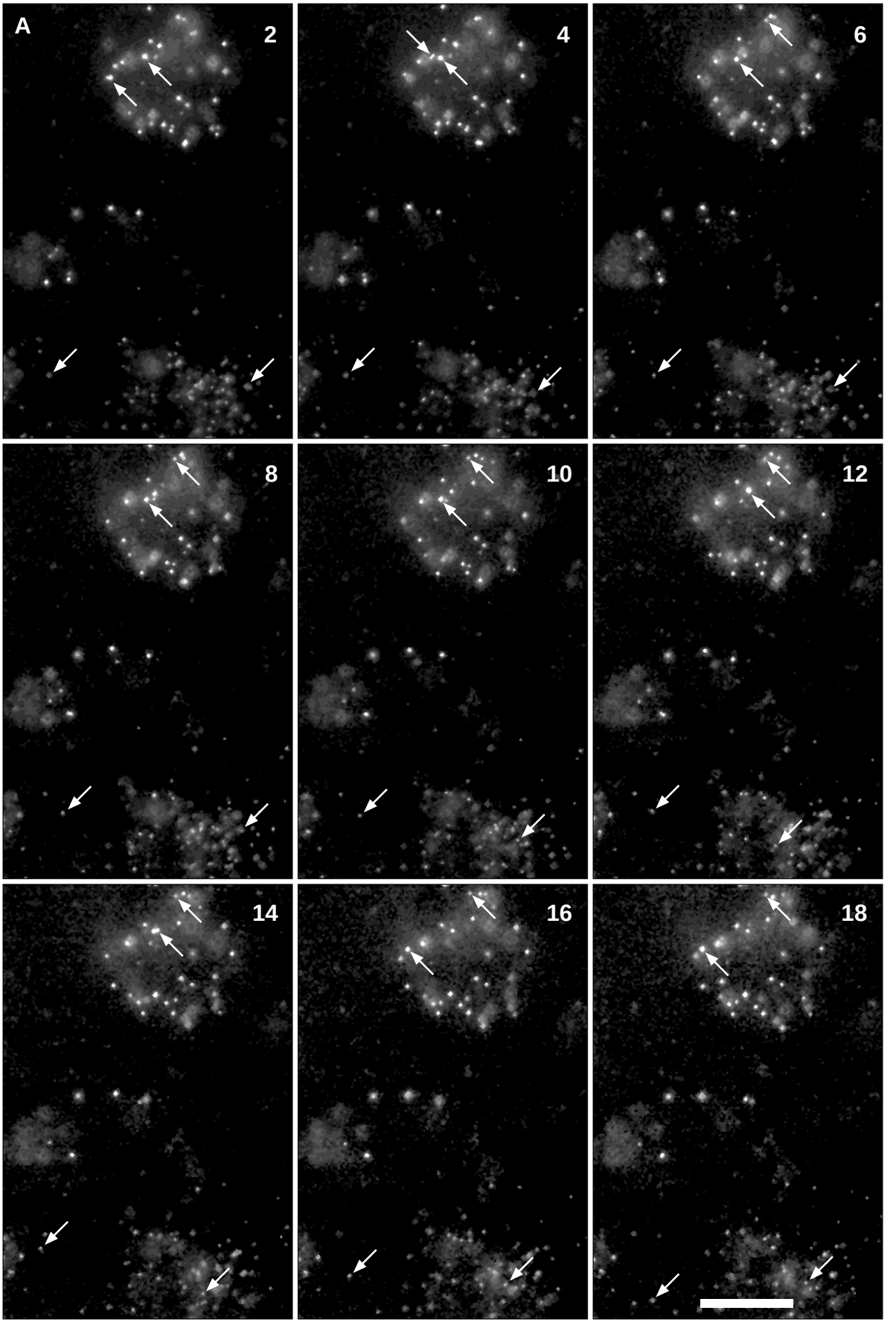
A
2
4
6
8
10
12
14
16
18

Table 1. Velocity of peroxisomes in CHO cells in vivo

	Control		SLO-permeabilised		Cytochalasin D		Nocodazole	
	20°C	37°C	20°C	37°C	20°C	37°C	20°C	37°C
Group 1	0.013±0.006	0.024±0.012	0.012±0.009	n.d.	0.013±0.005	0.020±0.01	0.012±0.007	0.018±0.009
Group 2	0.12±0.06	0.26±0.17	0.11±0.08	n.d.	0.07±0.03	0.20±0.11	-	-

Velocity measurements were performed in control, SLO-permeabilised, cytochalasin D (1 μg/ml) treated and in nocodazole (10 μg/ml) treated CHO cells at 20 and 37°C. Velocities are given in μm/second ± s.e.m. (n.d., not determined).

catalase, the endogenous peroxisomal marker (Fig. 5B). These results demonstrate, first, that the low molar ratio of fluorescein to FL of about 1.5 is sufficient to clearly mark peroxisomes in vivo and, second, that the ability of FL to be imported is not considerably diminished by the labeling although the reaction predominantly utilises ε-amino groups of lysine residues one of which is an essential part of the SKL-targeting signal. Immediately after microinjection the cells reveal a high background fluorescence due to nonimported Fluos-FL, which impairs the microscopic identification of peroxisomes. The nonimported marker, however, is largely removed from the cytoplasm within 3-4 hours after which time peroxisomes become clearly visible.

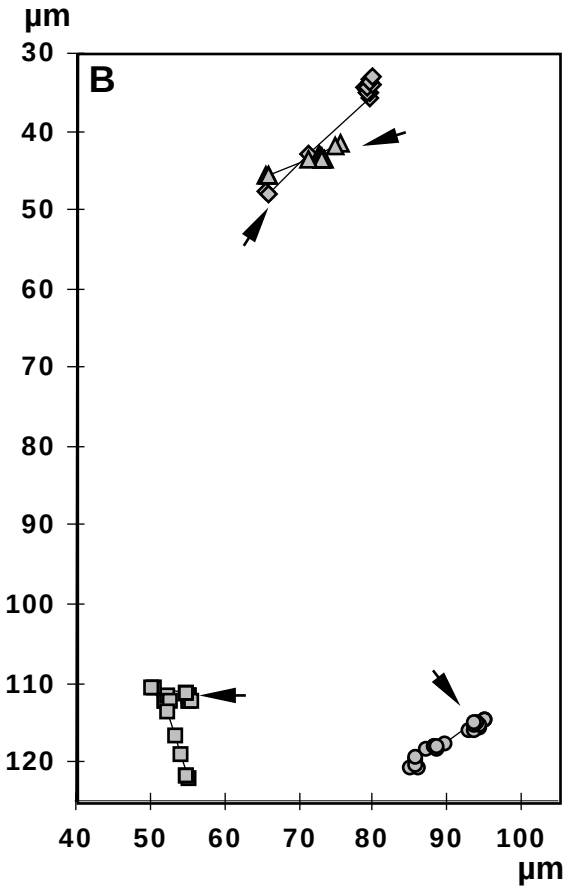

Fig. 6. Time-lapse imaging of Fluos-FL marked peroxisomes of cultured CHO cells. Fluos-FL was microinjected into cultured CHO cells and 24 hours later peroxisome movements were analysed by fluorescence microscopy. A time series is shown consisting of 9 consecutive images which were taken at 1 minute intervals. Four peroxisomes were selected (arrows), the relative intracellular position of which could be observed in all images of the time series (A). The intracellular routes of the four selected peroxisomes which differ in direction and length are presented graphically (B) by superimposing the 20 images of the entire time series (pixel units were converted into a μm scale).The left upper corner of the images shown in (A) represents the center of the coordinate axis. Arrowheads mark the beginning of the time series. Bar, 20 μm.

Intracellular peroxisome movement

Peroxisomes were inspected under the fluorescence microscope 24 hours after microinjection. During a period of 10 minutes a set of twenty images was acquired at intervals of 30 seconds without changing the plane of focus in between. Nine consecutive images taken at 1 minute intervals are shown in Fig. 6A. The series reveals that nearly all peroxisomes alter their relative position during this time period. Some peroxisomes move within the focal plane and some others leave or enter it at any given time. Within this 10 minute period no preferential direction of movement was recognised (see Fig. 11). Detailed velocity analysis of peroxisomal movement performed both at 20°C and 37°C revealed two groups of peroxisomes. At 20°C group 1 peroxisomes, which comprised the majority of organelles, moved with a constant but slow average velocity of 0.013 μm/second. Velocities ranged between 0.009-0.02 μm/second. In contrast to that, group 2 peroxisomes moved in a saltatory manner, i.e. a given peroxisome largely retains its relative intracellular position for a certain time period before moving rapidly and in a linear direction. Approximately 10-15% of the total peroxisomal population belong to this group. The average velocity of the saltations was 0.12 μm/second and exhibited great variations ranging between 0.05-0.9 μm/second. The two types of peroxisomal movement become more evident from the plot shown in Fig. 6B which exhibits the time dependent course of the intracellular movement of some organelles selected from Fig. 6A. Only those peroxisomes that stayed within the focal plane during the entire time series and that saltated transiently were selected. At 37°C group 1 and group 2 peroxisomes moved with average velocities of 0.024 μm/second and 0.26 μm/second, respectively (Table 1). Thus, group 2 peroxisomes moved 2.2 times faster at 37°C compared to 20°C.

Energy requirements of peroxisomal motility

In order to study the energy requirements for peroxisomal motility, cells were treated with NaN_3 and 2-deoxyglucose in glucose free medium 30 minutes before microscopic inspection. As shown previously (Soto et al., 1993) this treatment in CHO cells effectively reduces the level of endogenous ATP to less than 5% of the control. Under these conditions peroxisomal motility was completely blocked (Fig. 7A) as during the observation period the organelles did not alter their relative cellular position (Fig. 7B). In additional experiments we investigated the nucleotide dependence of peroxisome motility in

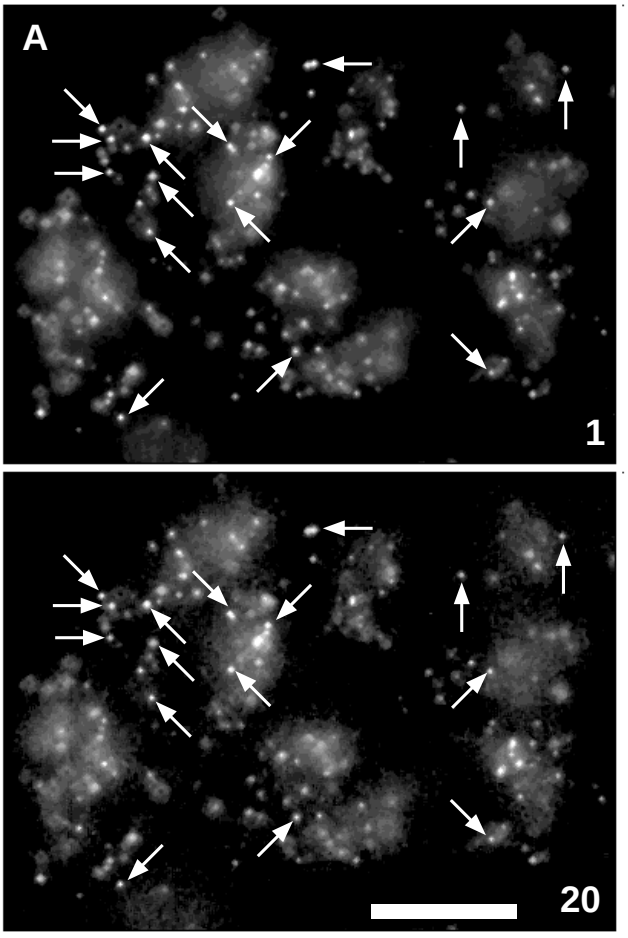

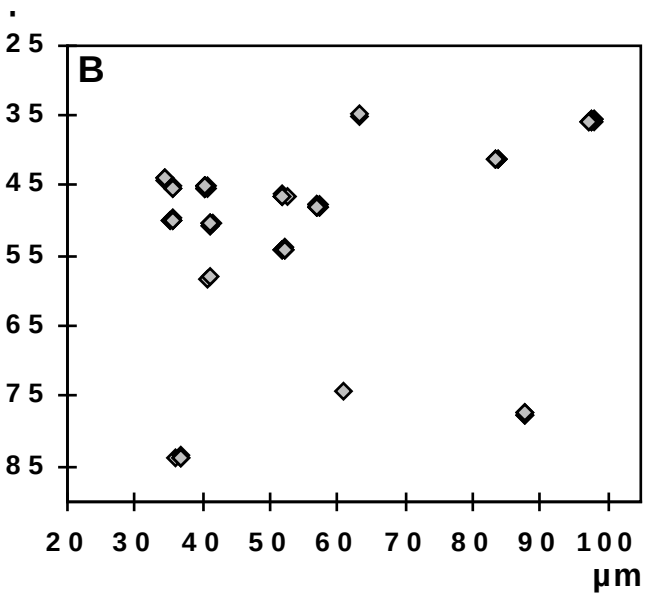

Fig. 7. ATP dependence of peroxisome movement. For ATP-depletion CHO cells were treated with NaN_3/2-deoxyglucose in glucose-free medium 30 minutes prior to time-lapse imaging of Fluos-FL marked peroxisomes. The relative intracellular position of selected peroxisomes (arrows) is compared on the first and last image of the time series (A). The immobilised state of selected peroxisomes under these deenergised conditions is graphically documented by superimposition of the 20 images of the time series (B). Pixel units were converted into a µm scale. Bar, 20 µm.

greater detail. To this end the cells were microinjected with Fluos-FL on the day before and permeabilised in a medium containing SLO as well as appropriate concentrations of ATP and GTP along with an ATP regenerating system in order to maintain the endogenous level of NTPs. Under these conditions again two groups of moving peroxisomes were observed of which group 2 peroxisomes showed saltatory movement (Fig. 8A). The velocities of these peroxisomal movements were virtually the same as those observed in intact cells (Table 1). The ATP-dependence of peroxisomal motility was analysed by omitting the ATP regenerating system but adding to the medium GTP and 1 mM AMP-PNP, a nonhydrolysable ATP analog. Immediately after incubating the cells in this medium analysis of peroxisome motility was started. Only within the first minutes was the movement of the peroxisomes detectable. Thereafter, organelle motility was diminished and completely ceased after 5-6 minutes, most likely as a result of the ongoing depletion of endogenous ATP (Fig. 8B).

Peroxisome association with microtubules

Dependency of peroxisomal motility on NTPs strongly suggests actin microfilaments and/or microtubules to be involved. The motor proteins of both of these cytoskeletal components have been shown to require ATP for their physiological function and both systems have been demonstrated to mediate organelle motility (for reviews see Walker and Sheetz, 1993; Ruppel and Spudich, 1995). Since our electron microscope studies clearly pointed towards the interaction of peroxisomes with microtubules, we first concentrated on this cytoskeletal component and its role in the translocation of peroxisomes. The microtubular network was depolymerised by nocodazole at a concentration of 10 µg/ml and the disappearance of microtubules was controlled by immunofluorescence (Fig. 9). The effect of nocodazole treatment on peroxisomal motility is illustrated in Fig. 10. The saltations spanning relatively large spatial distances were no longer observed suggesting that this type of movement is mediated by the microtubular system. However, the slow movements leading to only minor dislocations of the organelles were still recognised. Their average velocity was 0.012 µm/second with maximal values of up to 0.027 µm/second, similar to the low velocity exhibited by the control group 1 peroxisomes (Table 1).

The close association of peroxisomes and microtubules as observed by electron microscopy (Figs 1-4) as well as by colocalising the fluorescence patterns of tubulin and FL (Fig. 11A) offered the possibility of directly correlating peroxisomal movement with distinct microtubules. Therefore, we coinjected TRITC-labeled tubulin and Fluos-FL in order to simultaneously visualise microtubules and their associated peroxisomes in vivo. In peripheral regions of the cell, where microtubules are less abundant than in the perikaryon, peroxisomal saltations were clearly demonstrated to be linked to distinct microtubular tracts (Fig. 11B,C).

Peroxisome association with actin filaments

In order to study the involvement of actin filaments with peroxisome motility, depolymerisation of microfilaments was

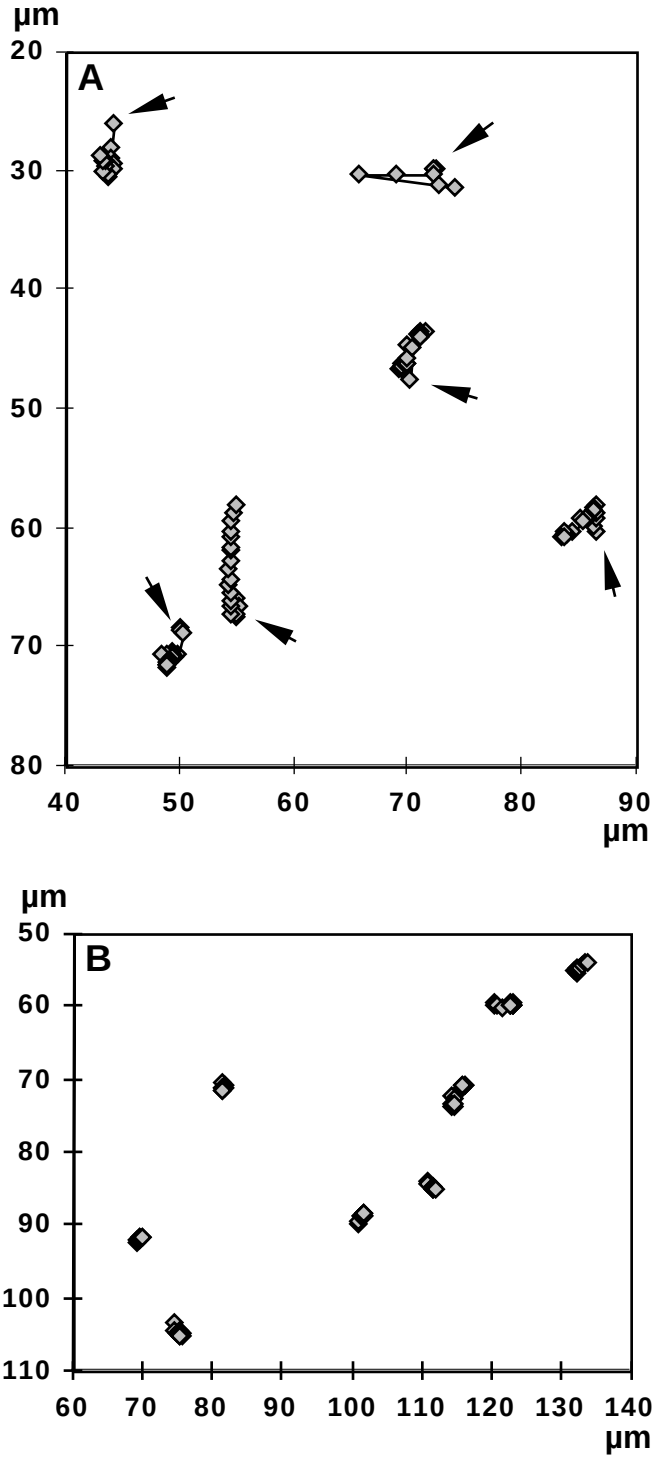

Fig. 8. ATP-dependence of peroxisome movement in permeabilised CHO cells. (A) CHO cells were microinjected with Fluos-FL and permeabilised with SLO 24 hours later. Appropriate NTP levels were maintained by incubating the cells in medium containing ATP, GTP and an ATP regenerating system. (B) ATP was depleted by omitting ATP and the ATP regenerating system and adding to the medium AMP-PNP (1 mM). Peroxisomal motility was analysed by time-lapse imaging of the fluorescence-labeled organelles starting 3 minutes after the addition of SLO. The images of the entire time series were superimposed and are illustrated graphically. Complete inhibition of peroxisome movement is documented for some selected organelles. Arrowheads mark the beginning of the time series.

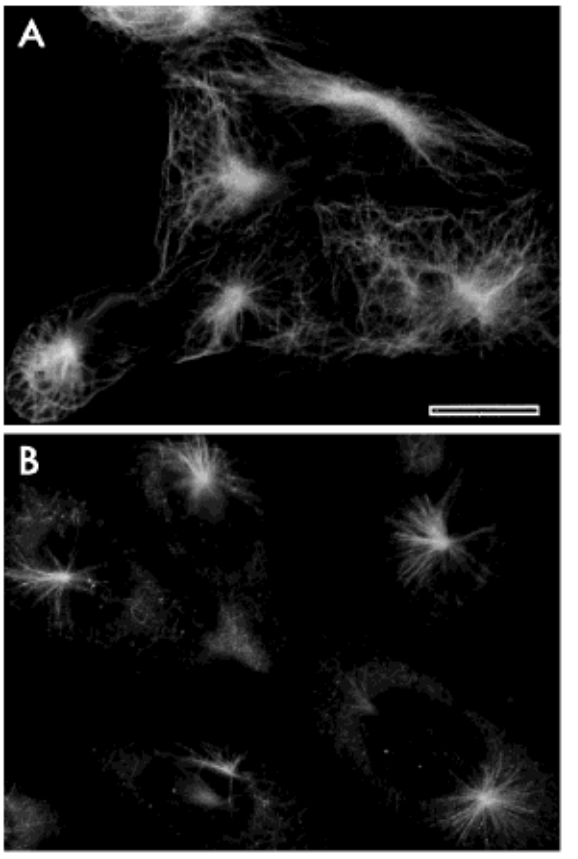

Fig. 9. Depolymerisation of microtubules of cultured CHO cells by nocodazole (10 µg/ml). Microtubular structures of controls (A) and nocodazole-treated (B) CHO cells were visualised by immunofluorescence using a monoclonal anti-α-tubulin antibody. The complex microtubule network is completely abolished and only a few short branches of microtubules are radiating from the microtubule organising center. Bar, 20 µm.

induced by 1 µg/ml cytochalasin D. Subsequently actin filaments were visualised by FITC-phalloidin. The typical assembly states of actin molecules including unbranched linear bundles, arcs and foci were seen. This concentration of cytochalasin D added to the culture medium was sufficient to largely abolish F-actin structures (Fig. 12). In contrast to nocodazole, however, this treatment had only a slight effect on peroxisomal motility. According to their style of movement the two groups of peroxisomes were still recognisable, but whereas movement of group 1 peroxisomes was practically the same as that in untreated cells, saltations of group 2 peroxisomes exhibited a velocity of 0.20 µm/second at 37°C and thus appeared to be reduced by about 25% compared to controls (Fig. 13; Table 1). Although peroxisomal motility is partially inhibited by the depolymerisation of actin microfilaments, these filaments only play a minor role in mediating peroxisomal motility.

DISCUSSION

Specificity of the system

Following either microinjection or selective permeabilisation of the plasma membrane FL is imported into peroxisomes of

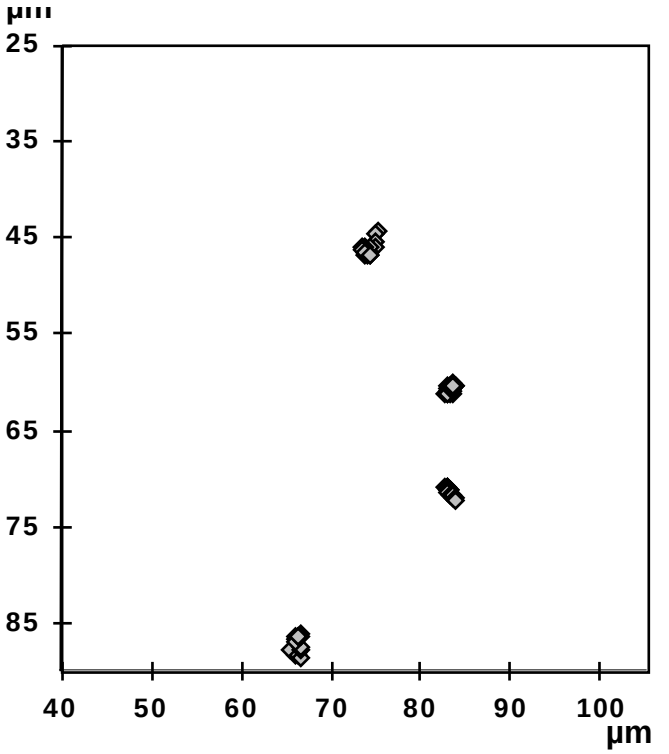

Fig. 10. Dependence of peroxisome saltations on the presence of intact microtubules. Graphical presentation of time-lapse imaging of Fluos-FL marked peroxisomes in cultured CHO cells 1 hour after treatment with 10 µg/ml nocodazole which selectively depolymerises the microtubular network. The relative intracellular position of four selected peroxisomes is followed throughout the time series of which 9 consecutive images are shown. Note that the saltatory movement of peroxisomes is no longer observed.

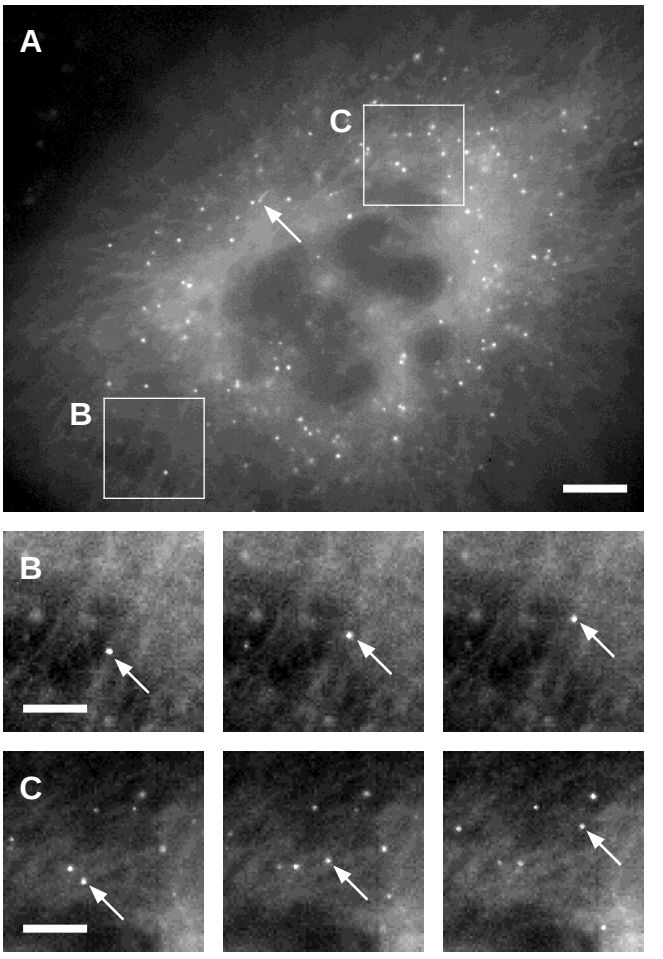

Fig. 11. Overlay of time-lapse images of cultured CHO cells at 37°C after comicroinjection of Fluos-FL and TRITC-labeled tubulin. For each time point two images were acquired consecutively for either fluorescence excitation. In the overview (A) a CHO cell is shown which exhibits distinct in vivo labeling of both peroxisomes and the dense microtubule network. Two peripheral cytoplasmic portions were selected and shown as enlarged image sequences (B and C) at three different time points after starting the series (B, 75, 105 and 135 seconds; C, 15, 30 and 60 seconds). Peroxisomes moving along microtubule tracks are marked with arrows in B and C. The arrow in A indicates a peroxisome moving quickly during image acquisition resulting in a fuzzy, tail-like appearance of the organelle. Note that the peroxisome in B moves towards the cell center whereas that in C towards the cell periphery. Bars: 10 µm (A); 5 µm (B and C).

various tissue culture cells (Walton et al., 1992; Soto et al., 1993). Consequently, fluorescence prelabeling of the import marker allowed us to visualise peroxisomes in vivo and to analyse their intracellular movement. Specific staining of peroxisomes was demonstrated by colocalisation of Fluos-FL with catalase which was used as an endogenous peroxisomal marker. Both Fluos-FL and catalase gave an identical punctate fluorescence pattern suggesting that the microinjected Fluos-FL is exclusively confined to peroxisomes.

Peroxisomal motility

The detailed analysis of peroxisomal motility by time lapse imaging and fluorescence microscopy revealed that according to their velocity peroxisomes may be classified into two distinct groups. About 85-90% of the total organelle population of a given cell belong to group 1 exhibiting low velocities of 0.013 or 0.024 µm/second, dependent on whether the analysis was performed at 20 or 37°C, respectively. This movement does not contribute to a considerable net organelle translocation in a distinct direction, but rather appears to be randomly oriented. Since it is not influenced by drugs that depolymerise actin filaments or microtubules, most likely it reflects thermal oscillation persisting as long as the organelles are not firmly attached to cytoskeletal structures. Peroxisomes of group 2 moved with an average velocity of 0.12 and 0.26 µm/second at 20 and 37°C, respectively, with maximal values of more than 2 µm/second. Thus, peroxisomes move 2.2 times faster at 37°C compared with 20°C. Gross (1973) studied the temperature dependence of fast axoplasmic transport in olfactory nerves of the garfish and reported on a linear increase of the transport rate between 10 and 28°C. The linear extrapolation of these values to 37°C predicts a 2.3-fold rate increase between 20 and 37°C which is in close agreement with the 2.2-fold increase found in our studies. This fast movement is saltatory and responsible for the net transport of peroxisomes. Most saltations are short-lived, but occasionally some of them could be followed over distances of more than 10 µm. They occur in both directions towards and away from the cell center suggesting two types of motor proteins to be involved, most

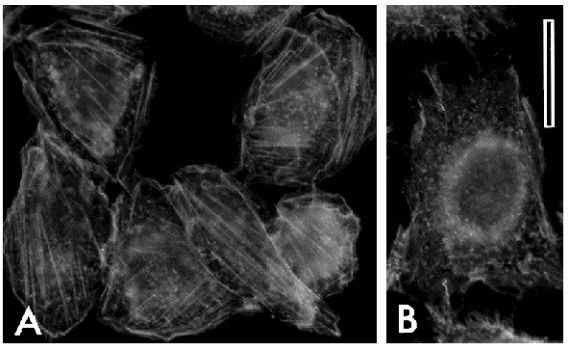

Fig. 12. Depolymerisation of actin microfilaments in cultured CHO cells by cytochalasin D (1 μg/ml). Control (A) and drug-treated (B) CHO cells were stained with FITC-phalloidin. Bar, 20 μm.

likely members of the cytoplasmic dynein and/or kinesin families, respectively (Vallee, 1993; Goodson et al., 1994). Using different cell systems similar observations on the movement of cell organelles other than peroxisomes were previously reported (Couchman and Rees, 1982; Schliwa, 1984; Gotoh et al., 1985; Leterrier et al., 1994) demonstrating saltatory movements to range from 0.5 to 5.0 μm/second with an average velocity of 1-2 μm/second.

In addition to these two types of movements a motionless state of peroxisomes was envisaged following complete depletion of metabolic energy. Such a 'frozen' state was also demonstrated on other cell organelles, e.g. rat brain mitochondria, and interpreted as a locking of the organelles to microtubules via ATP-dependent MAPs and/or motor proteins (Schroer and Sheetz, 1991; Brady and Pfister, 1991; Yu et al., 1992; Leterrier et al., 1994).

Interaction of peroxisomes with microtubules

Whereas the slow movement of peroxisomes was not at all influenced by anticytoskeletal drugs, the rapid saltations were completely abolished by the specific antimicrotubular agent nocodazole suggesting that this type of movement is mediated by microtubules. Motility of axoplasmic organelles, of mitochondria or melanophore pigment granules similarly is influenced by nocodazole (Couchman and Rees, 1982; Allen et al., 1985; Haimo and Thaler, 1994). In addition, our kinetic data obtained by the simultaneous labeling of microtubules and peroxisomes provide evidence for the intracellular transport of peroxisomes along microtubular tracks, and thereby confirm the electron microscope observations that not only reveal close association between peroxisomes and microtubules but moreover indicate the interaction of more than one microtubule with a given peroxisome. Furthermore, these microtubules do not necessarily traverse in parallel. Interaction of axoplasmic organelles with more than one microtubule has been demonstrated convincingly by ultrastructural and kinetic studies in vitro (Smith et al., 1975, Schnapp et al., 1986). On the one hand, these multiple interactions may increase both the duration and stability of contacts and hence may be important for rapid transport over longer distances. On the other hand, the interaction of one peroxisome with two nonparallel microtubules at the same time could give rise to rapid changes in the shape of the organelle.

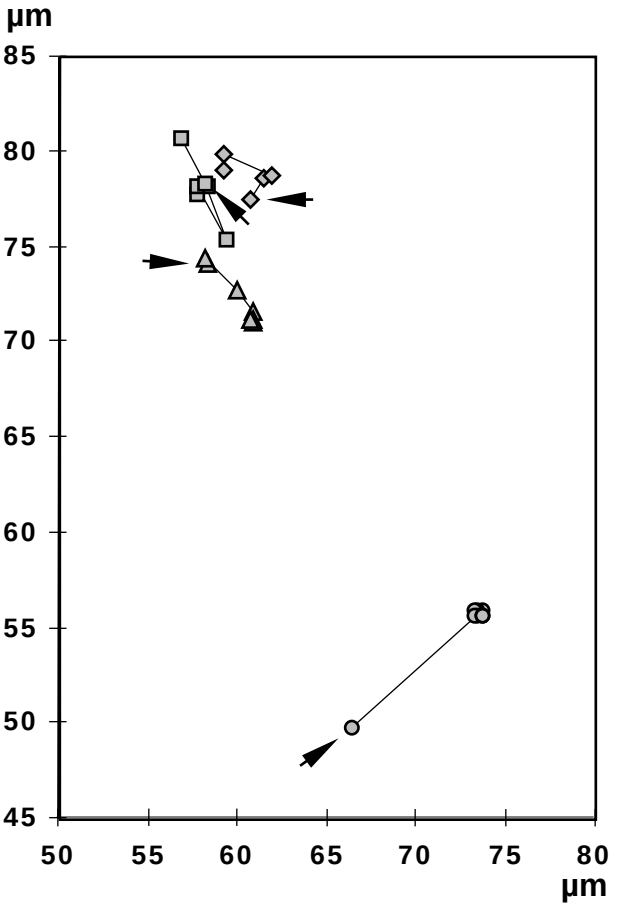

Fig. 13. Time-lapse imaging analysis of peroxisome movement in cultured CHO cells after depolymerisation of actin microfilaments by cytochalasin D. The intracellular position of three selected peroxisomes is followed throughout the entire time series and is presented graphically on a μm scale. Saltatory peroxisome movement still is observed although single saltations were reduced in length compared to controls by about 25% (see text). Arrowheads mark the beginning of the time series.

Interactions of peroxisomes with actin filaments

The intracellular transport of peroxisomes was influenced not only by nocodazole treatment but also by cytochalasin D-induced actin depolymerisation although the effect of the latter treatment was less pronounced. Saltations still were observed but, in comparison to the untreated controls their average velocity at 37°C was reduced by about 25%. To date, it is not clear whether this cytochalasin D induced effect points to a direct or indirect interaction of peroxisomes with actin filaments. Actin dependent movement of various types of squid axoplasmic organelles along neuronal as well as skeletal muscle actin filaments was recently described (Kuznetsov et al., 1992; Langford et al., 1994). The organelles investigated include axoplasmic vesicles, mitochondria and tubulovesicular structures (for a review see Langford, 1995). Although the function of this actin dependent organelle motility is not known, it seems to be coordinated with the microtubule system and possibly fulfills a subservient role in organelle transport.

Role of peroxisomal-microtubular associations

The bidirectional transport of peroxisomes away from and

towards the cell center may guarantee either the even distribution of the organelles throughout the cytoplasm or, as observed in polarised proximal tubular cells of the kidney, their specific basolateral location. Indeed, this view is supported by the observation that after nocodazole inhibition of tubulin polymerisation for longer periods (24 hours) peroxisomes tend to accumulate in the perikaryon of CHO cells (not shown). In line with these data Mori et al. (1981) emphasised a microtubule-based regulation of cell organelle distribution in rat hepatocytes during mitosis which has been induced by partial hepatectomy. All cell organelles including mitochondria, lysosomes and peroxisomes displayed an identical distribution pattern during the various stages of mitosis.

Peroxisome transport may also be important for the regulated degradation of the organelles which is believed to proceed via autophagy and lysosomal degradation (Yokota et al., 1993). Mori et al. (1982) reported on the preferential pericanalicular location of lysosomes in normal adult rat liver. Correspondingly, autophagic vacuoles containing segregated peroxisomes are regularly observed near the bile canaliculus of rat liver after the administration of peroxisome proliferators (Just et al., 1989).

In addition, interactions of cell organelles with microtubules have been demonstrated to be responsible for the formation and maintenance of tubular networks such as the endoplasmic reticulum (Dabora and Sheetz, 1988; Allan and Vale, 1994) and to some minor extent endosomes (Parton et al., 1991), lysosomes (Hollenbeck and Swanson, 1990) and the Golgi complex (Rogalski and Singer, 1984; Marks et al., 1994). Tubulovesicular membrane structures were reconstituted in vitro and a model for their generation was proposed (Dabora and Sheetz, 1988). Point contacts between membranes and nonparallel microtubules translocate along the microtubules thus providing the force to draw out tubular branches. A similar mechanism may be envisaged for the formation of complex tubular peroxisomes as they occur in late stages of cellular differentiation in sebaceous glandular cells (Figs 3, 4).

A major aspect of peroxisome biogenesis is the formation of new peroxisomes which is believed to occur by budding off from preexisting organelles (Lazarow and Fujiki, 1985). Vesiculation of membranes, a common process in living cells, is usually triggered by coat proteins, e.g. clathrin, COP I, COP II (Brown and Greene, 1991; Rothman, 1994; Barlow et al., 1994) or caveolin which may be involved in the invagination of the plasma membrane of many cell types (Anderson, 1993). In some rare cases, however, endocytosis has been reported to proceed without the participation of a protein coat (Hansen et al., 1991). So far, no coated structures have been implicated with peroxisomal buds and therefore the question as to the mechanism of peroxisomal budding remains open. The involvement of cytoskeletal components in this process may not be excluded.

We thank Dr S. Bhakdi, University of Mainz, and Dr U. Stewart, University of Darmstadt, for their generous gifts of SLO as well as anti-actin and anti-tubulin antibodies, respectively. We also thank Drs T. Hyman and R. Tournebize, EMBL Heidelberg, for samples of TRITC-labeled tubulin. Finally we are greatly indebted to Dr F. Wieland, University of Heidelberg, and Dr D. Weiss, University of Rostock, for valuable comments upon reading the manuscript. The work was supported by the Deutsche Forschungsgemeinschaft, SFB 352.

REFERENCES

Allan, V. and Vale, R. D. (1994). Movements of membrane tubules along microtubules in vitro: evidence for specialised sites of motor attachments. *J. Cell Sci.* **107**, 1885-1897.

Allen, L. A., Hope, L., Raetz, C. R. and Thieringer, R. (1994). Genetic evidence supporting the role of peroxisome assembly factor (PAF)-1 in peroxisome biogenesis. Polymerase chain reaction detection of a missense mutation in PAF-1 of Chinese hamster ovary cells. J. Biol. Chem. **269**, 11734-11742.

Allen, R. D., Weiss, D. G., Hayden, J. A., Brown, D. T., Fujiwake, H. and Simpson, M. (1985). Gliding movement of and bidirectional transport along single native microtubules from squid axoplasm: evidence for an active role of microtubules in cytoplasmic transport. *J. Cell Biol.* **100**, 1736-1752.

Anderson, R. G. (1993). Caveolae: where incoming and outgoing messengers meet. *Proc. Nat. Acad. Sci. USA* **90**, 10909-10913.

Aniento, F., Emans, N., Griffiths, G. and Gruenberg, J. (1993). Cytoplasmic dynein-dependent vesicular transport from early to late endosomes (published erratum appears in *J. Cell Biol.* (1994) **124**, 397). *J. Cell Biol.* **123**, 1373-1387.

Ansorge, W. and Pepperkok, R. (1988). Performance of an automated system for capillary microinjection into living cells. *J. Biochem. Biophys. Meth.* **16**, 283-292.

Barlow, C., Orci, L., Yeung, T. T., Hosobuchi, M., Hamamoto, S., Salama, N., Rexach, M. F., Ravazzola, M., Amherdt, M. and Scheckman, R. (1994). COP II: a membrane coat formed by Sec proteins that drive vesicle budding from the endoplasmic reticulum. *Cell* **77**, 895-908.

Bhakdi, S., Weller, U., Walev, I., Martin, E., Jonas, D. and Palmer, M. (1993). A guide to the use of pore-forming toxins for controlled permeabilisation of cell membranes. *Med. Microbiol. Immunol.* **182**, 167-175.

Bomsel, M., Parton, R., Kuznetsov, S. A., Schroer, T. A. and Gruenberg, J. (1990). Microtubule- and motor-dependent fusion in vitro between apical and basolateral endocytic vesicles from MDCK cells. *Cell* **62**, 719-731.

Brady, S. T. and Pfister, K. K. (1991). Kinesin interactions with membrane bounded organelles in vivo and in vitro. *J. Cell Sci. Suppl. 14*, 103-108.

Brown, V. I. and Greene, M. I. (1991). Molecular and cellular mechanisms of receptor-mediated endocytosis. *DNA Cell Biol.* **10**, 399-409.

Couchman, J. R. and Rees, D. A. (1982). Organelle-cytoskeleton relationships in fibroblasts mitochondria, Golgi apparatus, and endoplasmic reticulum in phases of movement and growth. *Eur. J. Cell Biol.* **27**, 47-54.

Dabora, S. L. and Sheetz, M. P. (1988). The microtubule-dependent formation of a tubulovesicular network with characteristics of the ER from cultured cell extracts. *Cell* **54**, 27-35.

Diestelkötter, P. and Just, W. W. (1993). In vitro insertion of the 22-kD peroxisomal membrane protein into isolated rat liver peroxisomes. *J. Cell Biol.* **123**, 1717-1725.

Erdmann, R. and Blobel, G. (1995). Giant peroxisomes in oleic acid-induced Saccharomyces cerevisiae lacking the peroxisomal membrane protein Pmp27p. *J. Cell Biol.* **128**, 509-523.

Goldfischer, S., Moore, C. L., Johnson, A. B., Spiro, A. J., Valsamis, M. P., Wisniewski, H. K., Ritch, R. H., Norton, W. T., Rapin, I. and Gartner, L. M. (1973). Peroxisomal and mitochondrial defects in the cerebro-hepato-renal syndrome. *Science* **182**, 62-64.

Goodson, H. V., Kang, S. J. and Endow, S. A. (1994). Molecular phylogeny of the kinesin family of microtubule motor proteins. *J. Cell Sci.* **107**, 1875-1884.

Gorgas, K. (1984). Peroxisomes in sebaceous glands. V. Complex peroxisomes in the mouse preputial gland: serial sectioning and three-dimensional reconstruction studies. *Anat. Embryol. Berl.* **169**, 261-270.

Gorgas, K. (1985). Serial section analysis of mouse hepatic peroxisomes. *Anat. Embryol. Berl.* **172**, 21-32.

Gotoh, H., Takenaka, T., Horie, H. and Hiramoto, Y. (1985). Organelle motility in rat pituitary clonal cells. I. Dynamic movements of intracellular organelles. *Cell Struct. Funct.* **10**, 233-243.

Gould, S. G., Keller, G. A. and Subramani, S. (1987). Identification of a peroxisomal targeting signal at the carboxy terminus of firefly luciferase. *J. Cell Biol.* **105**, 2923-2931.

Gross, G. W. (1973). The effect of temperature on the rapid axoplasmic transport in C-fibers. *Brain Res.* **56**, 359-363.

Haimo, L. T. and Thaler, C. D. (1994). Regulation of organelle transport: Lessons from color change in fish. *BioEssays* **16**, 727-733.

Hansen, S. H., Sandvig, K. and van Deurs, B. (1991). The preendosomal compartment comprises distinct coated and noncoated endocytic vesicle populations. *J. Cell Biol.* **113**, 731-741.

Herr, S., Bastian, T., Pepperkok, R., Boulin, C. and Ansorge, W. (1993). A fully automated image acquisition and analysis system for low light level fluorescence microscopy. *Meth. Mol. Cell. Biol.* **4**, 164-170.

Höhfeld, J., Veenhuis, M. and Kunau, W. H. (1991). PAS3, a Saccharomyces cerevisiae gene encoding a peroxisomal integral membrane protein essential for peroxisome biogenesis. *J. Cell Biol.* **114**, 1167-1178.

Hollenbeck, P. J. and Swanson, J. A. (1990). Radial extension of macrophage tubular lysosomes supported by kinesin. *Nature* **346**, 864-866.

Hyman, A., Drechsel, D., Kellogg, D., Salser, S., Sawin, K., Steffen, P., Wordeman, L. and Mitchison, T. (1991). Preparation of modified tubulins. *Meth. Enzymol.* **196**, 478-485.

Just, W. W., Gorgas, K., Hartl, F.-U., Heinemann, P., Salzer, M. and Schimassek, H. (1989). Biochemical effects and zonal heterogeneity of peroxisome proliferation induced by perfluorocarboxylic acids in rat liver. *Hepatology* **9**, 570-581.

Keller, G. A., Gould, S., Deluca, M. and Subramani, S. (1987). Firefly luciferase is targeted to peroxisomes in mammalian cells. *Proc. Nat. Acad. Sci. USA* **84**, 3264-3268.

Kuznetsov, S. A., Langford, G. M. and Weiss, D. G. (1992). Actin-dependent organelle movement in squid axoplasm. *Nature* **356**, 722-725.

Langford, G. M., Kuznetsov, S. A., Johnson, D., Cohen, D. L. and Weiss, D. G. (1994). Movement of axoplasmic organelles on actin filaments assembled on acrosomal processes: Evidence for a barbed-end-directed organelle motor. *J. Cell Sci.* **107**, 2291-2298.

Langford, G. M. (1995). Actin- and microtubule-dependent organelle motors: interrelationships between the two motility systems. *Curr. Opin. Cell Biol.* **7**, 82-88.

Lazarow, P. B., Shio, H. and Robbi, M. (1980). Biogenesis of peroxisomes and the peroxisome reticulum hypothesis. In *31st Mosbach Colloquium on Biological Chemistry of Organelle Formation* (ed. W. Bücher, H. Seebald and H. Weiss), pp. 187-206. Springer Verlag, New York.

Lazarow, P. B. and Fujiki, Y. (1985). Biogenesis of peroxisomes. *Annu. Rev. Cell Biol.* **1**, 489-530.

Leterrier, J. F., Rusakov, D. A., Nelson, B. D. and Linden, M. (1994). Interactions between brain mitochondria and cytoskeleton: evidence for specialised outer membrane domains involved in the association of cytoskeleton-associated proteins to mitochondria in situ and in vitro. *Microsc. Res. Technol.* **27**, 233-261.

Marks, D. L., Larkin, J. M. and McNiven, M. A. (1994). Association of kinesin with the Golgi apparatus in rat hepatocytes. *J. Cell Sci.* **107**, 2417-2426.

Matteoni, R. and Kreis, T. E. (1987). Translocation and clustering of endosomes and lysosomes depends on microtubules. *J. Cell Biol.* **105**, 1253-1265.

McCammon, M. T., Dowds, C. A., Orth, K., Moomaw, C. R., Slaughter, C. A. and Goodman, J. M. (1990). Sorting of peroxisomal membrane protein PMP47 from Candida boidinii into peroxisomal membranes of Saccharomyces cerevisiae. *J. Biol. Chem.* **265**, 20098-20105.

Mori, M., Enomoto, K., Saatoh, M. and Onoe, T. (1981). Translocation of hepatocyte lysosomes following partial hepatectomy and its inhibition by colchicine. *Exp. Cell Res.* **131**, 25-30.

Mori, M., Satoh, M. and Novikoff, A. B. (1982). Cytochemical and electron microscopic demonstration of organelle translocation and the inhibition of such translocation by colchicine during the mitosis of rat hepatocytes. *Exp. Cell Res.* **141**, 277-282.

Parton, R. G., Dotti, C. G., Bacallao, R., Kurtz, I., Simons, K. and Prydz, K. (1991). pH-induced microtubule-dependent redistribution of late endosomes in neuronal and epithelial cells. *J. Cell Biol.* **113**, 261-274.

Rapp, S., Soto, U. and Just, W. W. (1993). Import of firefly luciferase into peroxisomes of permeabilized Chinese hamster ovary cells: a model system to study peroxisomal protein import in vitro. *Exp. Cell Res.* **205**, 59-65.

Rasure, J., Williams, C., Argiro, D. and Sauer, T. (1990). A visual language and software development environment for image processing. *Int. J. Imaging Systems Technol.* **2**, 183-199.

Rogalski, A. A. and Singer, S. J. (1984). Associations of elements of the Golgi apparatus with microtubules. *J. Cell Biol.* **99**, 1092-1100.

Roscher, A. A. and Rolinski, B. (1992). Peroxisomal disorders in man. *Cell Biochem. Funct.* **10**, 201-207.

Rothman, J. E. (1994). Mechanism of intracellular protein transport. *Nature* **372**, 55-63.

Ruppel, K. M. and Spudich, J. A. (1995). Myosin motor function: Structural and mutagenic approaches. *Curr. Opin. Cell Biol.* **7**, 89-93.

Schliwa, M. (1984). Mechanisms of intracellular organelle transport. *Cell Muscle Motil.* **5**, 1-82.

Schnapp, B. J., Vale, R. D., Sheetz, M. P. and Reese, T. S. (1986). Microtubules and the mechanism of directed organelle movement. *Ann. NY Acad. Sci.* **466**, 909-918.

Schroer, T. A. and Sheetz, M. P. (1991). Two activators of microtubule-based vesicle transport. *J. Cell Biol.* **115**, 1309-1318.

Schutgens, R. B., Heymans, H. S., Wanders, R. J., van den Bosch, H. and Tager, J. M. (1986). Peroxisomal disorders: a newly recognised group of genetic diseases. *Eur. J. Pediatr.* **144**, 430-440.

Shimozawa, N., Tsukamoto, T., Suzuki, Y., Orii, T., Shirayoshi, Y., Mori, T. and Fujiki, Y. (1992). A human gene responsible for Zellweger syndrome that affects peroxisome assembly. *Science* **255**, 1132-1134.

Smith, D. S., Järlfors, U. and Cameron, B. F. (1975). Morphological evidence for the participation of microtubules in axonal transport. *Ann. NY Acad. Sci.* **253**, 472-506.

Soto, U., Pepperkok R., Ansorge, W. and Just, W. W. (1993). Import of firefly luciferase into mammalian peroxisomes in vivo requires nucleoside triphosphates. *Exp. Cell Res.* **205**, 66-75.

Subramani, S. (1993). Protein import into peroxisomes and biogenesis of the organelle. *Annu. Rev. Cell Biol.* **9**, 445-478.

Tan, X., Waterham, H. R., Veenhuis, M. and Cregg, J. M. (1995). The Hansenula polymorpha PER8 gene encodes a novel peroxisomal integral membrane protein involved in proliferation. *J. Cell Biol.* **128**, 307-319.

Tsukamoto, Miura, T. S. and Fujiki, Y. (1991). Restoration by a 35K membrane protein of peroxisome assembly in a peroxisome-deficient mammalian cell mutant. *Nature* **350**, 77-81.

Vallee, R. (1993). Molecular analysis of the microtubule motor dynein. *Proc. Nat. Acad. Sci. USA* **90**, 8769-8772.

Walker, R. A. and Sheetz, M. P. (1993). Cytoplasmic microtubule-associated motors. *Annu. Rev. Biochem.* **62**, 429-451.

Walton, P. A., Gould, S. J., Feramisco, J. R. and Subramani, S. (1992). Transport of microinjected proteins into peroxisomes of mammalian cells: inability of Zellweger cell lines to import proteins with the SKL-tripeptide peroxisomal targeting signal. *Mol. Cell. Biol.* **12**, 531-541.

Yokota, S., Himeno, M., Roth, J., Brada, D. D. and Kato, K. (1993). Formation of autophagosomes during degeneration of excess peroxisomes induced by di-(2-ethylhexyl)phthalate treatment. II. Immunocytochemical analysis of late autophagosomes. *Eur. J. Cell Biol.* **62**, 372-383.

Yu, H., Toyashima, I., Steuer, E. R. and Sheetz, M. P. (1992). Kinesin and cytoplasmic dynein binding to brain microsomes. *J. Biol. Chem.* **267**, 20457-20464.

Zaar, K., Hartig, F., Fahimi, H. D. and Gorgas, K. (1984). Peroxisomal aggregates forming large stacks in the lipid segment of the canine kidney. *Acta Histochem.* (suppl.) **29**, 165-168.

(Received 10 August 1995 - Accepted 10 January 1996)

Note added in proof

We would like to indicate that Schrader et al., *Eur. J. Cell Biol.* (in press) recently obtained some indications that microtubules may determine the peroxisome shape.